


AUTHOR QUERY FORM


	<p>Journal: CAR</p> <p>Article Number: 5704</p>	<p>Please e-mail or fax your responses and any corrections to:</p> <p>E-mail: corrections.essd@elsevier.sps.co.in</p> <p>Fax: +31 2048 52799</p>
---	---	--

Dear Author,

Please check your proof carefully and mark all corrections at the appropriate place in the proof (e.g., by using on-screen annotation in the PDF file) or compile them in a separate list. To ensure fast publication of your paper please return your corrections within 48 hours.

For correction or revision of any artwork, please consult <http://www.elsevier.com/artworkinstructions>.

Any queries or remarks that have arisen during the processing of your manuscript are listed below and highlighted by flags in the proof. Click on the 'Q' link to go to the location in the proof.

Location in article	Query / Remark: click on the Q link to go Please insert your reply or correction at the corresponding line in the proof
<p>Q1 </p>	<p>Highlights are 3–5 bullet points, no more than 85 characters per bullet point. Please provide it in correct format. For more information, see www.elsevier.com/researchhighlights.</p>
<p>Q2</p>	<p>Please provide significance of italic values in Table 3.</p>

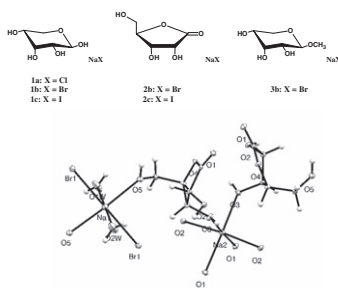
Thank you for your assistance.

Graphical abstract

Sodium halide complexes of ribose derivatives and their unusual crystal structures

pp xxx–xxx

Mátyás Czugler*, István Pintér



Research highlights

- Crystalline complexes of D-ribose, D-ribo-1,4-lactone and methyl β-D-ribofuranoside with sodium halogenides were synthesized and three crystal structures determined ► The D-ribo-1,4-lactone complexes have varying stoichiometries and water content ► The crystal structures of sodium halogenide complexes display regular cation coordination ► The methyl β-D-ribofuranoside 1:1 complex does not contain water and has unusual coordination ► The hydrated complexes have extensive hydrogen bonding while only meager HB contacts are in the non-hydrated one ► Such complexes can be easily prepared in solid state reactions in a ball mill.





Contents lists available at ScienceDirect

Carbohydrate Research

journal homepage: www.elsevier.com/locate/carres



Sodium halide complexes of ribose derivatives and their unusual crystal structures

Mátyás Czugler^{a,*}, István Pintér^b^aChemical Research Center, Institute of Structural Chemistry, Hung. Acad. Sci., Pusztaszeri u. 59-67, Budapest H-1025, Hungary^bEötvös Loránd University, Chemical Institute, Department of Organic Chemistry, Structural Chemistry and Biology Laboratory, Budapest 1117, Hungary

ARTICLE INFO

Article history:

Received 31 January 2011

Received in revised form 7 March 2011

Accepted 8 March 2011

Available online xxx

This paper is dedicated to Professor András Lipták on the occasion of his 75th birthday

Keywords:

Ribose derivatives

Sodium halide complexes

X-ray crystal structures

ABSTRACT

Crystalline complexes of D-ribose, D-ribo-1,4-lactone and methyl β-D-ribofuranoside with sodium halides were synthesized and some of their crystal structures determined. Crystal structures of two lactone complexes and a methyl β-D-ribofuranoside reveal the mode of the salt binding and the intricate interplay of cation coordination and hydrogen bonding in these complexes. When complexed with NaBr, the ribopyranoside is in the ¹C₄ shape whereas ribose with no salt present has the ⁴C₁ shape. It is also demonstrated that such complexes can be easily prepared in solid state reaction using a ball mill.

© 2011 Published by Elsevier Ltd.

1. Introduction

Complexes of disaccharides, cyclodextrins, and oligosaccharides with various metal salts have been known for some time.¹ Curiously enough, these complexes have been seldom studied despite their obvious biological and dietary implications such as for the important, simple oral rehydration therapy. In the case of monosaccharides, particularly, only few examples with alkali metal salts have been reported.^{1–7,11–14} Ribose is no exception: crystalline complexes with sodium salts have not been described for either D-ribose (**1**) or its derivatives. Ribose itself could also be considered understudied from a structural standpoint. Only recently was its crystal structure reported.⁸

Recently, during the production of D-ribo-1,4-lactone (**2**) one of us (IP) isolated a new complex of **2** with sodium bromide (**2b**).⁹ In that new complex, physical properties, such as solubility, melting point, and optical rotation were found to deviate from the known data of D-ribo-1,4-lactone synthesized first by E. Fischer.¹⁰ The composition of the compound was established by microanalysis, IR, and ¹H NMR spectroscopy as a 1:1 complex of the two components. Further experiments led to the isolation of a new complex of methyl β-D-ribofuranoside with sodium bromide (**3b**).⁴

Increasing interest in the role of D-ribose and its derivatives in biological processes prompted us to examine the formation and the structure of their complexes with sodium halides. Beforehand bis(sucrose) tris(sodium iodide) trihydrate and the dihydrate of the sodium bromide complex of sucrose were characterized by single crystal X-ray diffraction around 1946.^{11,12} Only few more structural studies were reported later. Gilli and co-workers,^{13,14} aside from reporting advanced structure models for the sucrose-NaBr·2H₂O system and the sodium iodide dihydrate 2:3:3 complex by X-ray crystallography also performed theoretical calculations on these crystals. Ferguson et al. described⁷ the correct crystal structure of the glucose-NaCl monohydrate complex, contrasting an earlier work that reported wrong unit cell, Laue- and space group.⁶ They also established isostructurality of the NaBr and NaI complexes, and also first described that the glucose-NaCl complex can be prepared by grinding the components with a pestle in a mortar. These studies, though initiated on different grounds can be somehow linked to oral rehydration therapy yielding to enhanced salt-sugar-water transport in men. A new complex of cellobiose·2NaI·2H₂O was also studied recently.¹⁵

2. Results and discussion

The syntheses of the complexes were performed under very simple reaction conditions.⁹ D-Ribose (**1**), D-ribo-1,4-lactone (**2**), and methyl β-D-ribofuranoside (**3**) in methanol or in acetone were mixed with each sodium salt under stirring at room

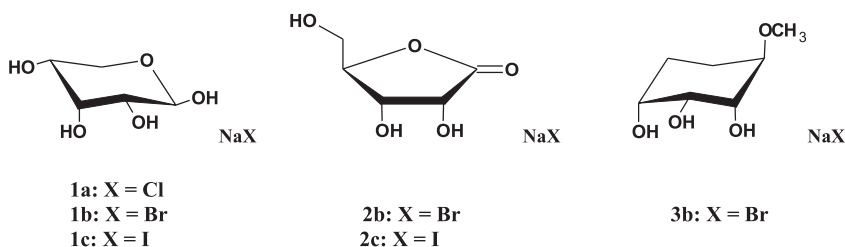
* Corresponding author. Tel.: +36 1 438 1161; fax: +36 1 325 7547.

E-mail addresses: mcz@chemres.hu (M. Czugler), pintis@elte.hu (I. Pintér).

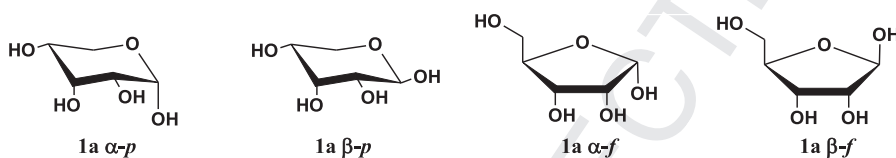
2 M. Czugler, I. Pintér / Carbohydrate Research xxx (2011) xxx–xxx

temperature to give the new complexes **1a–1c** and **2c**, respectively. In almost all cases the sugar and the salt dissolved within 15–30 min. The crystalline complexes were precipitated with an appropriate solvent as ethyl acetate or acetone. Crystals of D-ribose-NaCl (**1a**) spontaneously separated from the solution. The crystalline products were purified by dissolving in methanol and precipitating with either ethyl acetate or acetone.

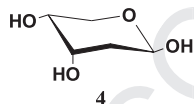
Crystals of new D-ribose-NaCl (**1a**), D-ribose-NaBr (**1b**), D-ribose-NaI (**1c**) and D-ribono-1,4-lactone-NaI (**2c**) were characterized with melting points, optical rotations, and determination of the halide content.



The structure of **1a** was corroborated also by ^1H and ^{13}C NMR spectra. In accordance with the values of the optical rotation, ^1H NMR spectra of the complex **1a** in aqueous solution exhibited the change of the concentration of the isomers of **1** into the equilibrium. After 1 h the concentration of β -pyranose (**1a** β -p) was found to be the highest (58.4%), while that of the α -pyranose (**1a** α -p) decreased to 21.9%. The equilibrium concentration of the β -furanose (**1a** β -f) and that of the α -furanose (**1a** α -f) were 12.4% and 7.3%, respectively.



The essential role of the HO-2 and HO-3, also attested by X-ray crystallography vide *infra*, was supported by the failure of the complexation of 2-deoxy-D-ribose (**4**) with NaBr.



In order to establish the exact structure of the molecules and to clear the nature of binding for such a small-size monosaccharide derivative and also to elucidate issues related to the solid state, systematic X-ray crystallographic studies have been started.

2.1. Single crystal X-ray diffraction

Herein we thus report the first crystal structures of the complexes **2b** and **2c** of D-ribono-1,4-lactone (**2**) with NaBr and NaI, respectively, as well as that of the complex **3b** of methyl β -D-ribofuranoside (**3**) with NaBr (Table 1). Crystals were grown by vapor diffusion using either acetone or ethyl acetate as anti-solvents into either a lactone-salt or riboside-salt solution in methanol.⁹ Well-developed single crystals grew within few days.

X-ray diffraction analysis of **2b** revealed the presence of a water molecule (Fig. 1). The structure determination shows that the crystal structure **2b** is typical catena-structure with differing cation, anion and molecular involvement of the components (Fig. 2).

Sodium cations occupy two non-equivalent crystallographic sites (special positions) thus giving rise to two different Na^+ cation kinds. From these properties of this crystal it follows that a real stoichiometry of the **2b** crystal is best described by 2:2:2.

One of the cations is in a salt bridge linking to the Br^- anion also coordinating to water and to the primary $-\text{OH}$ of the ribonolactone,

while the other one is fully shielded from the anion, a frequent phenomenon in hydrated salt structures such as, for example, in Ref. 7. It is, however, remarkable that the secondary $-\text{OH}$ groups of the furanoid ring solely coordinate this second sodium cation site. Both Na^+ cations are six-coordinated with comparable coordination geometries (cf. Table 2).

Cations are fused into two independent alternating ionic sheets along the planes at $\{x, y, 0\}$ and $\{x, y, \frac{1}{4}\}$, comprised by the hydrated

salt sheet and the cationic sheet fully shielded by D-ribono-1,4-lactone layers (Fig. 2), respectively.

Space group $C22_1$ permits the development of perfect C_2 -symmetric polymeric chains and obviously water uptake is useful in complementing the anion coordination sphere. Hydrogen bonding plays only a supplementary role as also shown by the H-atom positions. These are always directed such that the lone pairs of the $-\text{OH}$ groups are readily accessible for coordination (cf. Supplementary data).

In contrast to **2b** crystal structure, **2c** (Fig. 3) shows a totally asymmetric unit cell and a space group lacking any but translational symmetries with a 2:1:1 lactone:salt:water stoichiometry. The only Na^+ cation is shielded by two D-ribono-1,4-lactone moieties. Thus, there is no salt bridge link between cation and anion and the Na^+ cation is also six-coordinated. A non-crystallographic 2-fold rotation axis appears in this structure but this will not be matured into a crystallographic symmetry in the $P1$ space group. Water uptake is also needed for this crystal to form and water, together with the primary $-\text{OH}$ group, is active in keeping Br^- off of the cation. Comparison of respective bonds in these furanoid moieties indicates comparable geometries in **2**,¹⁶ in **2b** and in **2c** thus demonstrating neutral sugar forms (Table 3).

A Cambridge Structural Database¹⁷ analysis shows that the expected C3–O3 bond length in furanose type structures has a mean

Table 1
Crystal data and structure refinement characteristics of **2b**, **2c**, and **3b**

	2b	2c	3b
Empirical formula	C ₅ H ₁₀ BrNaO ₆	C ₁₀ H ₁₈ NaO ₁₁	C ₆ H ₁₂ BrNaO ₅
Formula weight	269.02	464.14	267.05
Temperature	93(2) K	295(2) K	93(2) K
Radiation, Mo K α , λ	0.71070 Å	0.71070 Å	0.71070 Å
Crystal system	Orthorhombic	Triclinic	Monoclinic
Space group	C222 ₁	P1	P2 ₁
Unit cell, a (Å)	7.333(2)	6.0080(12)	7.1795(13)
b (Å)	9.548(3)	6.0473(11)	6.0318(10)
c (Å)	25.7513(1)	11.4790(16)	10.8500(16)
α (°)	90	83.418(7)	90
β (°)	90	76.858(7)	96.192(8)
γ (°)	90	77.597(9)	90
Volume (Å ³)	1803.1(7)	395.71(12)	467.12(13)
Z	8	1	2
Density (calcd) Mg/m ³	1.982	1.95	1.9
Absorption coefficient, μ	4.603 mm ⁻¹	2.105 mm ⁻¹	4.434 mm ⁻¹
Crystal color	Colorless	Colorless	Colorless
Crystal description	Prism	Brick	Plate
Crystal size (mm)	0.35 × 0.30 × 0.30	0.32 × 0.24 × 0.22	0.38 × 0.28 × 0.07
Absorption correction	Empirical	Numerical	Numerical
Max/min transmission	1.000/0.589	0.742/0.637	0.832/0.272
θ -range data collection (°)	3.16 ≤ θ ≤ 27.48	3.46 ≤ θ ≤ 33.14	3.25 ≤ θ ≤ 34.97
Reflections collected	20576	30598	31184
Completeness to 2 θ	0.999	0.998	0.986
Independent reflections, R_{int}	2073, 0.033	5822, 0.022	3958, 0.059
Reflections $I > 2\sigma(I)$	2047	5821	3862
Data/restraints/parameters	2073/0/132	5822/3/209	3958/1/149
Goodness-of-fit on F^2	1.126	1.165	1.179
Extinction coefficient	0.00064(15)	0.0044(11)	—
Flack parameter	0.009(7)	0.007(8)	0.023(8)
Final R for $[I > 2\sigma(I)]$ R_1 , wR^2	0.0157, 0.0380	0.0184, 0.0428	0.0336, 0.0590
R indices (all data) R_1 , wR^2	0.0160, 0.0381	0.0184, 0.0428	0.0353, 0.0595
Max. and mean shift/esd	0.001; 0.000	0.001; 0.000	0.001; 0.000
Largest diff. peak/hole e Å ⁻³	0.33/−0.30	0.37/−0.40	0.94/−0.53

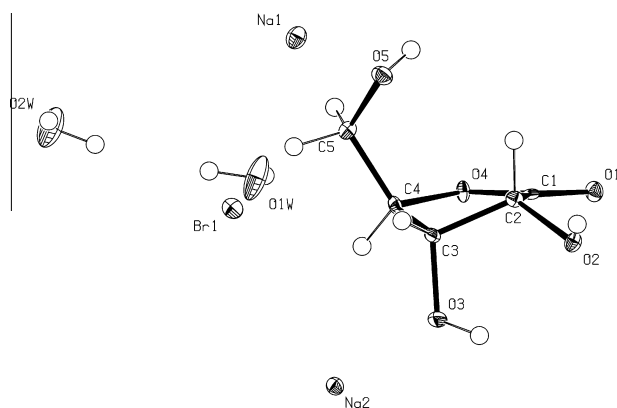


Figure 1. Asymmetric unit in the **2b** crystal structure with 50% probability displacement ellipsoids.

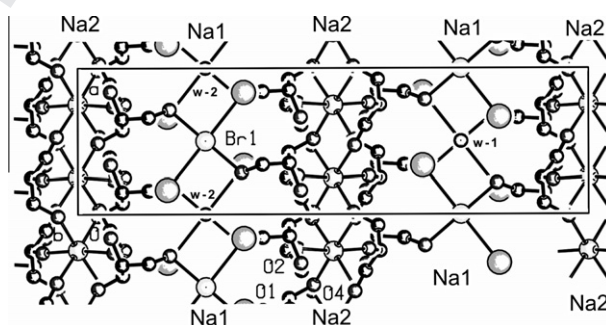


Figure 2. Infinite sheet structures in **2b** showing isolated Na⁺ ion layers involving water and direct anion/cation contacts as well as fully separated Na⁺ ion layers shielded by D-ribose-1,4-lactone arrays. Atom coding is shown for some Na, Br, ribose O, and water molecules while H atoms are omitted for clarity.

bond length around 1.41 Å thus the value in **2b** can be regarded as significantly deviating.

Packing in **2c** is less intriguing than in **2b** but also maintains dominating ionic interactions and additional strong hydrogen bridges (cf. Supplementary data). Common to both **2b** and **2c** is the sixfold cation coordination. This formal equivalence to the number of ligating O atoms to 18-crown-6 complexes is realized through the symmetric coordination polyhedron in **2b** and in an only slightly distorted one in **2c**. Na⁺ cation distances from the planes of two equatorial and an axial ligand atom show a shorter (1.34 Å) and a longer value (1.52 Å) in **2b**. The shorter value is for the Na⁺ cation bound by solely secondary O atoms, while the other is for the mixed coordination sphere. Similarly short distances

Table 2
Coordination distances for **2b**, for **2c**, and for **3b** (in Å)

	2b	2c	3b
Na2–O3 ^{a#}	2.359(2)	Na1–O21	2.347(2)
Na2–O1 ^{b#}	2.388(2)	Na1–O22	2.402(1)
Na2–O2 ^{c#}	2.418(2)	Na1–O11 ^f	2.436(2)
		Na1–O32	2.390(2)
Br1–Na1 [#]	3.117(1)	Na1–O31 ^g	2.421(2)
Na1–O1w ^d	2.291(2)	Na1–O12	2.455(2)
Na1–O5 ^{e#}	2.405(1)		
Na1–O2w ^e	2.267(3)		
		Br1–Na1	3.076(1)
		Na1–O5 ⁱ	2.661(2)
		Na1–O4 ⁱ	2.483(2)
		Na1–O4 ^h	2.463(2)
		Na1–O3	2.421(2)
		Na1–O3 ^h	2.461(2)
		Na1–O4 ⁱ	2.507(3)
		Na1–O4 ^h	2.704(2)

Symmetry codes to generate equivalent atoms: in **2b**: a = x, −y, −z + 1; b = x + 1, −y, −z + 1; c = x + 1/2, −y + 1/2, −z + 1; d = x + 1/2, −1, y + 1/2, z; e = x + 1/2, −1, y + 1/2, −1, z; in **2c**: f = x − 1, y, z + 1; g = x, y, −1, z + 1; in **3b**: h = 2 − x, y − 1/2, 1 − z; i = x, y − 1, z.

[#] These distances are replicated by the twofold symmetry.

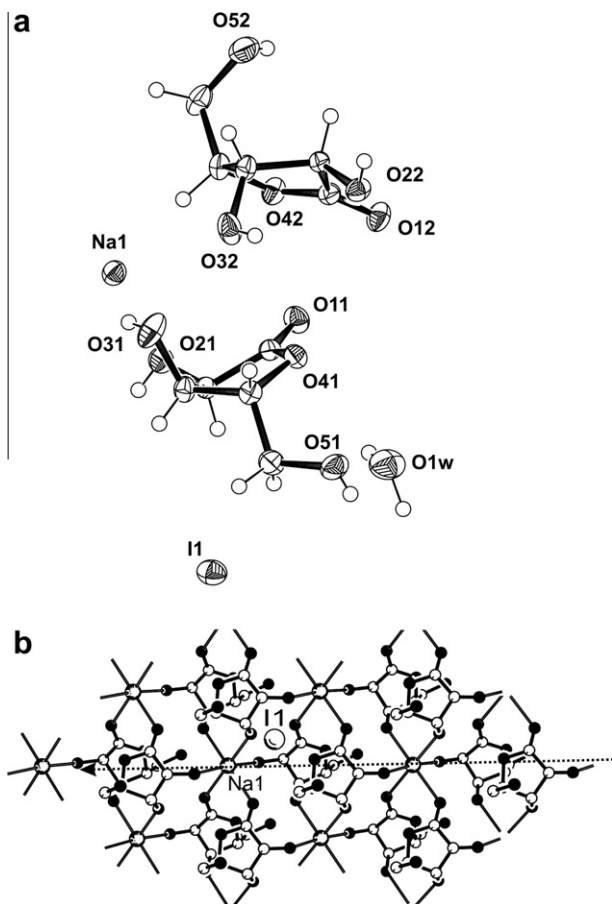


Figure 3. (a) ORTEP style plot of the **2c** asymmetric unit content showing heteroatomic numbering (50% probability displacement ellipsoids). (b) The isolated Na^+ from its counter-ion and showing an approximate non-crystallographic twofold axis relating lactone rings (dotted line).

Table 3
Bond lengths^c (Å) of **2**,¹⁶ **2b** and **2c**

Bond	2	2b	2c^a	2c^b	Mean
O1–C1	1.203	1.206	1.204	1.206	1.205
O2–C2	1.403	1.410	1.402	1.413	1.407
O3–C3	1.417	1.433	1.424	1.420	1.424
O4–C4	1.467	1.486	1.472	1.472	1.474
O4–C1	1.354	1.341	1.334	1.330	1.340
O5–C5	1.431	1.430	1.417	1.425	1.426
C1–C2	1.510	1.522	1.524	1.513	1.517
C2–C3	1.525	1.525	1.529	1.526	1.526
C3–C4	1.538	1.523	1.521	1.529	1.528
C4–C5	1.516	1.514	1.508	1.507	1.512

2c has two independent lactone molecules in the asymmetric unit. Standard uncertainty values are uniformly 0.001 Å for **2**,¹⁶ 0.002 Å for **2b** O–C bonds and 0.002–3 Å for the C–C ones, 0.002 Å for **2c** O–C bonds and 0.002–3 Å for the C–C ones.

from the like planes in **2c** are 1.32 and 1.36 Å. Thus, the three pairs of oxygens ligating Na^+ cations in the sixfold manner display an exaggerated pseudo-crown like binding. These structures probably present the minimal steric and electronic conditions for non-covalent organized binding for Na^+ . Another observation pertains to the pseudo-symmetric arrangements of the lactone ligands around the translation dependent sodium sites (Fig. 3b), lending a rather regular arrangement in a non-orthogonal crystal lattice. The lactone rings form an integral part of the catena-structure.

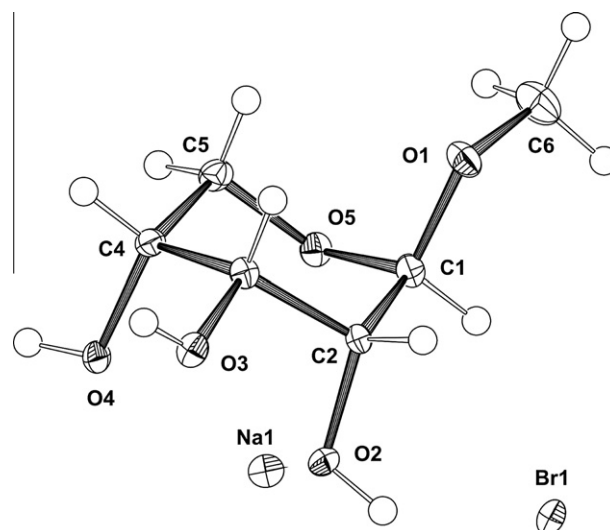


Figure 4. 50% Probability displacement ellipsoids plot of the asymmetric unit of the **3b** complex with atomic numbering.

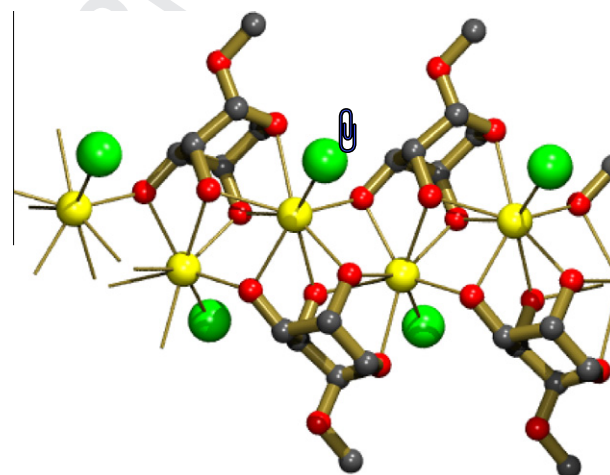


Figure 5. An excerpt from the **3b** crystal structure showing the salt binding region over the secondary –OH surface, with atom color coding but omitting all H atoms for clarity.

Crystal structure **3b** has 1:1 stoichiometry for **3**: NaBr and is deviating from the other two in that there is no water in this crystal (Fig. 4). H-bonding only plays a subordinate role here in a way of complementing the obviously more stern ionic interactions. Sodium cation is basically six-coordinated as far as the shortest distances in **3b** to six O atoms go. Longer close contacts between the anion and the cation and another O atom do exist, too. It is also interesting that neighboring Na^+ cations approach each other at 3.515(2) Å distance. Na^+ is sitting in the mid of a distorted polyhedron made from oxygen atoms and the anion (Fig. 5). As before secondary –OH groups dominate in these interactions and actually function much like a ‘solvation sphere’ toward the salt-sheet.

2.2. Ring puckering, sodium cation binding, and the H-bridge patterns

2.2.1. Ring shapes of the furanose ring

Cremer and Pople¹⁸ ring puckering analysis by the aid of PLATON¹⁹ to symmetrical forms of five-membered rings shows that

Table 4

Ring puckering parameters of the **2b** and **2c^a** ribofuranose rings as compared for the **2** crystal structure¹⁶

	Q ₍₂₎ (Å)	Φ ₍₂₎ (°)	P (°)	τ (°)	Δ (°)	Form
2b	0.309(2)	95.5(3)	184.4(2)	31.5(1)	368.9	² T ₃
2c^a	0.346(2)	100.3(2)	190.2(2)	35.0(1)	380.4	E ₃
2c^a	0.302(2)	95.5(3)	184.3(2)	30.7(1)	368.6	² T ₃
2	0.38	99.2	188.6	38.5	377.1	E ₃

For Q₍₂₎ and Φ₍₂₎ definitions see: Ref. 18, P and τ pseudo rotation parameters: Ref. 20, Δ is defined in Ref. 21.

^a Compound **2c** has two independent lactone rings in its asymmetric unit.

the furanose rings are either twisted on the C2–C3 bond or with C3 on the flap forms (Table 4). This latter is the ring shape in the uncomplexed **2** suggesting that these rings can adapt to the steric and electronic conditions of the salt complexation via even the relative slight adjustments possible in their overall shape. In other words one can state that this ring is preformed to complexation. This of course is in agreement with earlier analyses by Angyal.² It is to be noted though that mainly due to the spatial constraints exerted by the largely predetermined geometry of the O4/C2 > C1=O1 group only minor puckering excursions are permitted, as a fit of the two lactone rings attests (see Supplementary Fig.).

2.2.2. Ring shapes of the pyranose ring

The puckering analysis¹⁹ shows the pyranose ring in **3b** adopting a shape similar to a chair (Table 5). Parameters for the ¹C₄-form are given (Table 5, second row). The minor deviation from the canonical C form^{19,22} may be thought of as a snapshot on the pseudo-rotation pathway traversing through slight twists toward the perfect ¹C₄ chair in **3b** (see Fig. 4). This is in a striking contrast to the parent ribopyranose that has a nearly ideal canonical ⁴C₁ chair form. The evolution of this unusual chair form may most probably be attributed to the sodium cation coordination furnishing another peculiar aspect of this complex chemistry.

As suggested by Angyal,² the *ax-eq-ax* (*aea*) sequences in pyranoses promote metal ion complexation. This clearly applies for **3b**

Table 5

Ring puckering parameters^{18,22} of the **3b** ribopyranose ring compared for the ribose **3^a** crystal structure⁸

	Q(Å)	(°)	Φ(°)	Form
3b^b	0.560(2)	6.1(2)	262(2)	¹ C ₄
3-1⁸	0.543(8)	3.0(8)	295(21)	⁴ C ₁
3-2⁸	0.619(8)	3.1(7)	25(15)	⁴ C ₁

^a Compound **3** has two independent molecules in its asymmetric unit of form I, which is the only form analyzed here.

^b Values correspond to C4 as pivot atom so as to yield to canonical description.

where the non-H substituents are C(2)–O(2): *ax*, C(3)–O(3): *eq* and C(4)–O(4): *ax*. The *ax-ax* disposition of both C(1)–O(1) and O(5)–Na(1) does not appear to hinder cation binding either. The adoption of the new ring shape as well as the facile coordination sphere of Na⁺ is complemented through a sheet-like organization of the ligand-cation environment (Fig. 5). The infinite *catena-structure* is apparent here, too, as is the eminent role of the secondary –OH groups lining up the salt-sheet surface. This layer of sodium ions can be plausibly visualized like a rolling stone over the undulating surface of the secondary –OH groups. The soft iodide anion attaches to the sides of this cation zigzag layer.

For a detailed overview of the H-bonding pattern the reader is referred to the Supplementary data. As to the general H-bonding tendency one should conclude that intermolecular contacts are mostly to the anions and to the water molecules. Only a few contacts between lactone and riboside are likely to correspond to hydrogen bonds.

2.3. Solid state reactions

We explored whether solvent-free preparation of such complexes is possible by carrying out initial attempts on **2b** with dry powders of **2** and of NaBr in a ball mill. A low-energy vibrator mill was used and the progress of the events was followed by X-ray powder diffraction of samples taken at regular intervals for a total grinding time of 1 h. Experiments on anhydrous mixtures of the

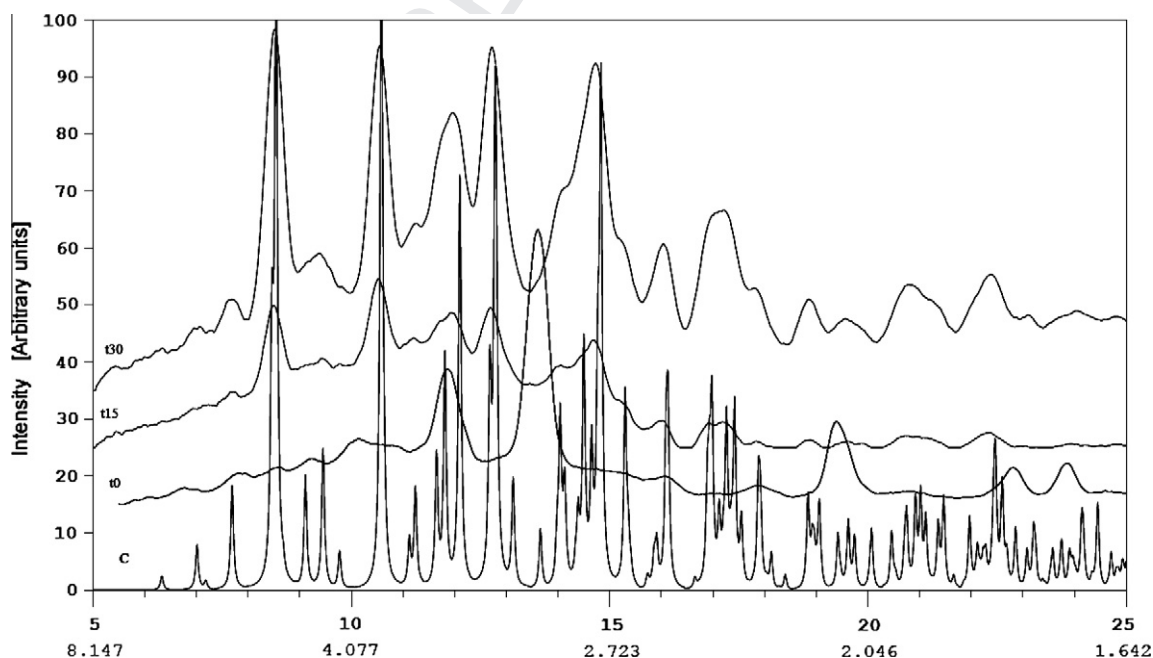


Figure 6. Calculated diffractogram based on the **2b** crystal structure (marked by C) as compared for the experimental powder diffractograms taken before the beginning of milling (*t*₀) and taken at 15 (*t*₁₅) and 30 min (*t*₃₀) intervals after. Intensity in arbitrary units, horizontal ticks show 2θ- and *d*-values (upper and lower figures, respectively).

reactants indicated only increasing amounts of amorphous substance in powder diffractograms (not shown). This may also be related to the relative low energy of the mill applied. On the other hand addition of a trace of water to the mixture (to about 0.5 g total powder mass was added 5–10 μL water) before grinding led to rapid evolution of the complex as witnessed by the sequence of powder diffractograms (Fig. 6).

These show that the reaction, as compared for the ideal diffractogram calculated from the single-crystal X-ray structure, is nearly complete after half of an hour and no traces of the original physical mixture are visible. It is also clear that in accord with a general reaction path idea for ball mill reactions²³ this very process goes through an amorphous intermittent state of the substances. Importance of the water involvement in **2b** is also indicated by these pilot experiments, with faint similarity to solvent drop grinding.²⁴

Thus, one can conclude that at least some of these complexes can be easily prepared in a 'green chemistry' fashion in short reaction times.

2.4. Summary

Carbohydrate derivatives seem to sustain an essential role both in the drug discovery²⁵ and modifications as well as in the formulation of drugs.²⁶ It did not escape our attention that these findings may bear direct or indirect relationships to the chemical behavior of some pharmaceutical additives in their solid state formulations.²⁶ Work is in progress to describe further models of such as the salt complexes described herein as well as other related derivatives. Common to these structures are the formation of more or less regular infinite layer structures. Secondary $-\text{OH}$ groups play a pivotal role and the involvement of the anion appears to be subordinate in the coordination of sodium cations. Bond valence model calculations^{27,28} also support the notion of highly regular and normal Na^+ -coordination spheres. In the crystal structures **2b**, **2c**, and **3b** the sum of the bond valences are consistently (1.18 and 1.24, 1.17 and 1.15) over one as expected for Na^+ .²⁹ The secondary $-\text{OH}$ groups generally appear on the top of the bond valences underlining their role in the cation binding. The individual bond valence numbers in these top ranges are by about 10% over and under 0.2, respectively. These figures agree rather well for Na^+ coordination in biological milieu as analyzed for a large sample of enzyme crystal structures,²⁹ perhaps underlining dietary implications for sugar-salt complexes (vide supra), too. The coordination volumes³⁰ seem to agree either with the presence of the anion in the coordination sphere and or with the compactness of the coordination (octahedral volumes of 22.7 and of 18.1 \AA^3 for **Na1** and **Na2** in **2b**, of 18.5 \AA^3 for **2c** and the larger polyhedron volume of 30.6 \AA^3 for **3b**). Normally large molecules, such as crown ethers or other polyhydroxy macrocycles as, for example, modified calix-arenes or pyrogallarenes³¹ are needed to effectively complex sodium salts. The crystal structures **2b**, **2c** and **3b** are also interesting in that respect that only rather small, neutral organic molecules are involved in forming these solid crystalline associations. Trivially they are inherently chiral and easy to obtain.

3. Experimental

3.1. General methods

Melting points were determined with Kofler micromelting apparatus and are uncorrected. For TLC precoated Merck Silica Gel 60 F254 plates were used and developed by charring with concd H_2SO_4 . Eluents are given in each experiment. Optical rotations were measured with a Zeiss Polamat A polarimeter. Nuclear magnetic resonance spectra were determined on a DRX-500 BRUKER

spectrometer. Assignment of ^1H and ^{13}C signals given is based on 2D-HSQC and 2D-HMBC spectra. Microanalysis was performed by the Microanalytical Laboratory of the Chemical Institute of Eötvös Loránd University. X-ray diffraction experiments were made on a Rigaku R-AXIS RAPID image plate diffractometer at low (93 K) and room temperature. This same machine was used recording powder diffractograms used for solid state reaction monitoring. Solid state reactions were affected in a Narva vibrator mill DDR-GM9458 type using either steel or agate balls in separate experiments.

3.2. Synthesis of complexes

3.2.1. D-Ribose-NaCl (1a)

To D-ribose (6.00 g, 40 mmol) in MeOH (25 mL) was added sodium chloride (2.34 g, 40 mmol) under stirring at room temperature. Under continuous stirring solids dissolved within some minutes, then crystals started to separate. The product was filtered to give white crystals (4.90 g) of the crude **1a** melting at 158–161 $^\circ\text{C}$. From the mother liquor an additional crop of crystals (2.14 g) was obtained increasing the total yield to 84.4%. Recrystallization of a sample afforded white crystals of the pure **1a**, mp 165–167 $^\circ\text{C}$; $[\alpha]_{\text{D}} -12.1$ (10'), $\rightarrow 4.5$ (1 h) (H_2O , c 3). Calcd from $\text{C}_5\text{H}_{10}\text{O}_5 \cdot \text{NaCl}$ $[\alpha]_{\text{D}} -14.2$. TLC (EtOAc-MeOH 9:1) revealed only one spot of D-ribose (R_f , 0.09). ^1H NMR (500 MHz, D_2O) δ 5.35 (d, 0.07H, J 3.8 Hz, H-1 α -f); 5.22 (d, 0.12H, J 1.9 Hz, H-1 β -f); 4.90 (d, 0.58H, J 6.5 Hz, H-1 β -p); 4.84 (d, 0.22H, J 2.0 Hz, H-1 α -p); 4.18–3.50 (overlapped signals of the pentose protons in the equilibrium). ^{13}C NMR (125 MHz, D_2O) δ 101.39, 96.70, 94.27, 93.94, 83.55, 82.93, 75.70, 71.43, 71.32, 70.86, 70.48, 69.61, 69.35, 67.77, 67.66, 63.59, 63.43, 62.96, 61.84. Anal. Calcd for $\text{C}_5\text{H}_{10}\text{ClNaO}_5$ (208.57): Cl, 17.00. Found: Cl, 16.42.

3.2.2. D-Ribose-NaBr (1b)

To a solution of D-ribose (0.50 g, 3.3 mmol) in MeOH (10 mL) was added sodium bromide (0.35 g, 3.4 mmol) under stirring at room temperature. Under continuous stirring solids dissolved within some minutes, then the mixture was diluted with ethyl acetate (15 mL). The precipitate was filtered and washed with ethyl acetate to give white crystals of **1b** (0.62 g, 72.1%), mp 179–181 $^\circ\text{C}$; $[\alpha]_{\text{D}} -11.3$ (H_2O , c 3). Calcd from $\text{C}_5\text{H}_{10}\text{O}_5 \cdot \text{NaBr}$ $[\alpha]_{\text{D}} -11.7$. TLC (EtOAc-MeOH 9:1) revealed only one spot of D-ribose (R_f , 0.09). Anal. Calcd for $\text{C}_5\text{H}_{10}\text{BrNaO}_5$ (253.02): Br, 31.58. Found: Br, 31.06.

3.2.3. D-Ribose-Nal (1c)

To a solution of sodium iodide (0.23 g, 1.53 mmol) in acetone (5 mL) D-ribose (0.23 g, 1.53 mmol) was added under stirring at room temperature. Under continuous stirring solids dissolved within some minutes, then the mixture was diluted with ethyl acetate (5 mL). The precipitate was filtered and washed with ethyl acetate to give white crystals (0.82 g, 82.6%) of pure **1c** melting at 136–138 $^\circ\text{C}$; $[\alpha]_{\text{D}} -7.8$ (10'), $\rightarrow 10.6$ (3 days) (H_2O , c 4.5). Calcd from $\text{C}_5\text{H}_{10}\text{O}_5 \cdot \text{NaI}$ $[\alpha]_{\text{D}} -10.7$. TLC (EtOAc-MeOH 9:1) revealed only one spot of D-ribose (R_f , 0.09). Anal. Calcd for $\text{C}_5\text{H}_{10}\text{INaO}_5$ (300.02): I, 42.30. Found: I, 41.99.

3.2.4. D-Ribono-1,4-lactone-Nal (2c)

To a solution of D-ribono-1,4-lactone (0.44 g, 3 mmol) in a mixture of acetone (5 mL) and MeOH (1 mL) sodium iodide (0.45 g, 3 mmol) was added under stirring at room temperature. Under continuous stirring solids dissolved within some minutes. Solvents were removed by distillation under reduced pressure and the crystalline residue was re-dissolved in acetone (5 mL). Dilution with ethyl acetate (15 mL) resulted in slow separation of pure **1c** in white crystals (0.64 g, 71.9%), mp 71–72 $^\circ\text{C}$; $[\alpha]_{\text{D}} +12.3$ (H_2O , c 4).

Calcd for $2C_5H_8O_5 \cdot NaI \cdot H_2O$ $[\alpha]_D +11.7$. Anal. Calcd for $C_{10}H_{18}NaO_{11}$ (464.14): I, 27.34. Found: I, 27.13.

3.3. Solid state reaction of 2 with NaBr

3.3.1. Dry milling

Equimolar amounts of **2** and NaBr of typically about 0.2–0.5 g were measured and homogenized by spatula mixing in an agate mortar for about 2–5 min. An aliquot powdery specimen was taken in an X-ray capillary. Remaining powder was transferred into 5 cm³ volume crucible of the vibrator mill and either steel or agate balls were applied for a total milling time of 1 h. Milling was stopped at every 15 min, material was scraped off the crucible walls, homogenized and minute amounts filled into X-ray capillaries. These capillaries were collected and subjected to 10–15 min X-ray exposures on the R-Axis RAPID diffractometer. The X-ray powder diffraction control showed that the anhydrous samples had increasing amorphous content, but also that the characteristic peaks of the first physically mixed sample were still visible after 1 h.

3.3.2. Wet milling

The above procedure was applied with the addition of 5–10 μ L water to about 0.5 g total mass of dry powder. Water was injected directly in the crucible after taking the 0 min powder sample. Subsequent procedure was identical as outlined above, with the early appearance of new peaks in the X-ray diffractograms.

Acknowledgments

Financial support by the Hungarian Research Fund (Grant No. OTKA T042642, K-75869 and K72973) and a diffractometer purchase grant from the National Office for Research and Technology (MU-00338/2003) are gratefully acknowledged. The European Union and the European Social Fund have provided financial support to the project under the grant agreement No. TÁMOP 4.2.1./B-09/KMR-2010-0003. Authors are grateful to Drs. Antal Csámpai for ¹H and ¹³C NMR spectra and István Sajó for redrawing Fig. 6. We also thank one of the referees of the paper for suggestions relating to the pseudo rotation pattern analysis in **3b** and for general advices.

Supplementary data

Crystallographic data excluding structure factors have been deposited with the Cambridge Crystallographic Data Centre, CCDC

No. 608195–608197 for **2b**, **2c** and **3b**, respectively. Copies of this information may be obtained free of charge from the Director, Cambridge Crystallographic Data Centre, 12 Union Road, Cambridge, CB2 1EZ, UK (fax: +44 1223 336033, e-mail: deposit@ccdc.cam.ac.uk or via: www.ccdc.cam.ac.uk). Supplementary data associated with this article can be found, in the online version, at doi:10.1016/j.carres.2011.03.014.

References

1. Rendleman, J. A., Jr. Complexes of Alkali Metals and Alkaline-Earth Metals with Carbohydrates In *Advance in Carbohydrate Chemistry*; Wolfrom, M. L., Tipson, R. S., Eds.; Academic Press: New York, 1967; Vol. 21, pp 209–271.
2. Angyal, S. J. Complexes of Metal Cations with Carbohydrates in Solution In *Advance in Carbohydrate Chemistry and Biochemistry*; Tipson, R. S., Horton, D., Eds.; Academic Press: New York, 1989; Vol. 47, pp 1–42.
3. Benner, K. et al On The Metal Binding Site of The Carbohydrates. In *Carbohydrates as Organic Raw Materials IV*; Praznik, W., Huber, A., Eds.; WUV-Universitätsverlag: Wien, 1998; pp 64–67.
4. Beevers, C. A.; Cochran, W. *Nature* **1946**, *157*, 872.
5. Rendleman, J. A., Jr. *J. Org. Chem.* **1966**, *31*, 1839–1845.
6. Cho, Y.; Honzatko, R. B. *Acta Crystallogr., Sect. C* **1990**, *46*, 587–590.
7. Ferguson, G.; Kaitner, B. B.; Connet, E.; Rendle, B. F. *Acta Crystallogr., Sect. B* **1991**, *47*, 479–484.
8. Sisak, D.; McCusker, L. B.; Zandomenighi, G.; Meier, B. H.; Blaeser, D.; Boese, R.; Schweizer, W. B.; Gilmour, R.; Dunitz, J. D. *Angew. Chem., Int. Ed.* **2010**, *49*, 4503–4505.
9. Pintér, I. *Pol. J. Chem.* **2005**, *79*, 323–328.
10. Fischer, E.; Piloty, O. *Ber* **1891**, *24*, 4214–4216.
11. Cochran, W. *Nature* **1946**, *157*, 231–233.
12. Beevers, C. A.; Cochran, W. *Proc. R. Soc. London, Ser. A* **1947**, *190*, 257–272.
13. Accorsi, C. A.; Bellucci, F.; Bertolasi, V.; Ferretti, V.; Gilli, G. *Carbohydr. Res.* **1989**, *191*, 91–104.
14. Accorsi, C. A.; Bellucci, F.; Bertolasi, V.; Ferretti, V.; Gilli, G. *Carbohydr. Res.* **1989**, *191*, 105–116.
15. Peralta-Inga, Z.; Johnson, G. P.; Dowd, M. K.; Rendleman, J. A., Jr.; Stevens, E. D.; French, A. D. *Carbohydr. Res.* **2002**, *337*, 851–888.
16. Kinoshita, Y.; Ruble, J. R.; Jeffrey, G. A. *Carbohydr. Res.* **1981**, *92*, 1–7. CSD REFcode: BAGZAK.
17. Allen, F. H. *Acta Crystallogr., Sect. B* **2002**, *58*, 380–388.
18. Cremer, D.; Pople, J. A. *J. Am. Chem. Soc.* **1975**, *97*, 1354–1358.
19. Spek, A. L. *Acta Crystallogr., Sect. D* **2009**, *65*, 148–155.
20. Rao, S. T.; Westhof, E.; Sundaralingam, M. *Acta Crystallogr., Sect. A* **1981**, *37*, 421–425.
21. Altona, C.; Geise, H. J.; Romers, C. *Tetrahedron* **1968**, *24*, 13–32.
22. Dowd, M. K.; French, A. D.; Reilly, P. J. *J. Carbohydr. Chem.* **2000**, *19*, 1091–1114.
23. Kaupp, G. *Cryst. Eng. Commun.* **2006**, *8*, 794–804.
24. Trask, A. V.; Shan, N.; Motherwell, W. D. S.; Jones, W.; Feng, S.; Tan, R. B. H.; Carpenter, K. J. *Chem. Commun.* **2005**, 880–882.
25. *Carbohydrate-Based Drug Discovery*; Wong, C.-H., Ed.; Wiley-VCH, 2003.
26. Byrn, S. R.; Xu, W.; Newman, A. W. *Adv. Drug Deliv. Rev.* **2001**, *48*, 115–136.
27. Brese, N. E.; O’Keeffe, M. *Acta Crystallogr., Sect. B* **1991**, *47*, 192–197.
28. Brown, I. D. *The Chemical Bond in Inorganic Chemistry: The Bond Valence Model*; Oxford University Press, 2002.
29. Nayal, M.; Di Cera, E. *J. Mol. Biol.* **1996**, *256*, 228–234.
30. Robinson, K.; Gibbs, G. V.; Ribbe, P. H. *Science* **1971**, *172*, 567–570.
31. Ahman, A.; Nissinen, M. *Chem. Commun.* **2006**, 1209–1211.